Jurnal Teknologi, 43(C) Dis. 2005: 67–83

BOUNDARY LAYER FLOW DUE TO A MOVING FLAT PLATE IN MICROPOLAR FLUID

MOHD ZUKI SALLEH[1], AZIZAH MOHD ROHNI[2] & NORSARAHAIDA AMIN[3]

Abstract. The mathematical model for a boundary layer flow due to a moving flat plate in micropolar fluid is discussed. The plate is moving continuously in the positive x-direction with a constant velocity. The governing boundary-layer equations are solved numerically using an implicit finite-difference scheme. Numerical results presented include the reduced velocity profiles, gyration component profiles and the development of wall shear stress. The results obtained, when the material parameter $K = 0$ (Newtonian fluid) showed excellent agreement with those for viscous fluids. Further, the wall shear stress increases with increasing K. For fixed K, the wall shear stress decreases and the gyration component increases with increasing values of n, in the range $0 \le n \le 1$ where n is a ratio of the gyration vector component and the fluid shear stress at the wall.

Keywords: Boundary layer, micropolar fluid, moving flat plate, Keller-box method, mathematical model

Abstrak. Pemodelan matematik bagi aliran lapisan sempadan terhadap plat rata bergerak telah dibincangkan. Satu plat bergerak berterusan dalam arah positif paksi-x dengan halaju tetap. Persamaan lapisan sempadan yang dihasilkan telah diselesaikan secara berangka dengan menggunakan skema beza terhingga tersirat. Keputusan berangka telah diberikan, ini termasuk profil halaju, profile komponen legaran dan perubahan tegasan ricih permukaan. Kajian ini menunjukkan bahawa keputusan bagi masalah dalam bendalir mikropolar berbanding dengan bendalir likat adalah sangat memuaskan apabila parameter bahan $K = 0$ (bendalir Newtonan). Seterusnya tegasan ricih permukaan meningkat dengan peningkatan nilai K. Untuk nilai K yang ditetapkan, didapati tegasan ricih permukaan menyusut dan kompenan legaran meningkat dengan peningkatan nilai n, dalam selang $0 \le n \le 1$, di mana n adalah nisbah kompenan vektor legaran dengan tegasan ricih bendalir pada permukaan.

Kata kunci: Lapisan sempadan, bendalir mikropolar, plat rata bergerak, kaedah Keller-box, pemodelan matematik

[1] Faculty of Mechanical Engineering, Kolej Universiti Kejuruteraan dan Teknologi Malaysia, Bandar MEC, 25500 Gambang, Kuantan, Pahang. E-mail: zuki@kuktem.edu.my
[2] Faculty of Quantitative Sciences, Universiti Utara Malaysia, 06010 UUM Sintok, Kedah. E-mail: r.azizah@uum.edu.my
[3] Department of Mathematics, Universiti Teknologi Malaysia, 81310 UTM Skudai, Johor. E-mail: nsarah@mel.fs.utm.my

1.0 INTRODUCTION

The boundary-layer flow over a moving continuous solid surface is important in several engineering processes. For example, materials manufactured by extrusion processes and heat-treated materials travelling between a feed roll and a wind-up roll or on conveyor belt possess the characteristics of a moving continuous surface. Sakiadis [1] first investigated the boundary-layer flow on a continuous solid surface moving at constant speed. Due to the entrainment of the ambient fluid, this boundary-layer flow is quite different from the Blasius flow past a flat plate. Sakiadis' theoretical predictions for Newtonian fluids were later corroborated experimentally by Tsou *et al.* [2]. Lee and Davis [3] investigated the laminar boundary layers on moving continuous surfaces while the turbulent boundary layer on a moving continuous plate was studied by Noor Afzal [4].

This paper will investigate the boundary layer flow due to a moving flat plate in both viscous and micropolar fluids. A micropolar fluid is one which contains suspensions of rigid particles such as blood, liquid crystals, dirty oil and certain colloidal fluids, which exhibits microstructure. The theory of such fluids was first formulated by Eringen [5]. The equations governing the flow of a micropolar fluid involve a microrotation vector and a gyration parameter in addition to the classical velocity vector field. This theory includes the effects of local rotary inertia and couple stresses and is expected to provide a mathematical model for the non-Newtonian behavior observed in certain man-made liquids such as polymeric fluids and in naturally occurring liquids such as animal blood. The theory of thermomicropolar fluids was also developed by Eringen [6] by extending the theory of micropolar fluids. A comprehensive review of micropolar fluid mechanics was given by Ariman *et al.* [7]. Their studies on the inadequacy of the classical Navier-Stokes theory to describe rheologically complex fluids such as liquid crystals, animal blood, etc., has led to the development of microcontinuum fluid mechanics as an extension of the classical theory. Many models have been proposed to take into account the mechanically significant microstructure of such fluids. Rees and Bassom [8] have considered the Blasius boundary layer flow of a micropolar fluid over a flat plate, while a similarity analysis of the flow and heat transfer past a continuously moving semi-infinite plane in micropolar fluid has been presented by Soundalgekar and Takhar [9].

This paper will also consider the problems of the boundary-layer flow. We derive and solve the full boundary layer equations. The analyses involve the pseudo-similarity transformation of the governing equations and the resulting nonlinear equations are then solved using an implicit finite difference scheme, the Keller-box method. The reduced velocity, reduced gyration component and development of wall shear stress are shown by means of graphs.

2.0 GOVERNING EQUATIONS

Consider the flow of a steady, laminar, incompressible micropolar fluid past an extensible sheet, which is moving continuously in the positive $\bar{x}$ – direction with an arbitrary surface velocity U. The orthogonal coordinates $\bar{x}, \bar{y}$ are measured along the sheet and, respectively, normal to it with the origin at a fixed point 0.

The full equations governing the two-dimensional steady flow of a micropolar fluid are (Ahmadi [10]):

$$\frac{\partial \bar{u}}{\partial \bar{x}} + \frac{\partial \bar{v}}{\partial \bar{y}} = 0 \tag{1}$$

$$\bar{u}\frac{\partial \bar{u}}{\partial \bar{x}} + \bar{v}\frac{\partial \bar{u}}{\partial \bar{y}} = -\frac{1}{\rho}\frac{\partial \bar{p}}{\partial \bar{x}} + \left(\mu + \frac{\kappa}{\rho}\right)\left(\frac{\partial^2 \bar{u}}{\partial \bar{x}^2} + \frac{\partial^2 \bar{u}}{\partial \bar{y}^2}\right) + \frac{\kappa}{\rho}\frac{\partial \bar{N}}{\partial \bar{y}} \tag{2}$$

$$\bar{u}\frac{\partial \bar{v}}{\partial \bar{x}} + \bar{v}\frac{\partial \bar{v}}{\partial \bar{y}} = -\frac{1}{\rho}\frac{\partial \bar{p}}{\partial \bar{x}} + \left(\mu + \frac{\kappa}{\rho}\right)\left(\frac{\partial^2 \bar{v}}{\partial \bar{x}^2} + \frac{\partial^2 \bar{v}}{\partial \bar{y}^2}\right) + \frac{\kappa}{\rho}\frac{\partial \bar{N}}{\partial \bar{y}} \tag{3}$$

$$\bar{u}\frac{\partial \bar{N}}{\partial \bar{x}} + \bar{v}\frac{\partial \bar{N}}{\partial \bar{y}} = -\frac{\kappa}{\rho\zeta} + \left(2\bar{N} + \frac{\partial \bar{u}}{\partial \bar{y}}\right) + \frac{\kappa}{\rho\zeta}\frac{\partial \bar{v}}{\partial \bar{x}} + \frac{\gamma}{\rho\zeta}\left(\frac{\partial^2 \bar{N}}{\partial \bar{x}^2} + \frac{\partial^2 \bar{N}}{\partial \bar{y}^2}\right) \tag{4}$$

Following Ahmadi [10], $(\bar{x}, \bar{y})$ are the coordinates parallel with and perpendicular to the flat surface, $(\bar{u}, \bar{v})$ is the velocity vector, $\bar{p}$ is the pressure, $\bar{N}$ is the component of the gyration vector normal to the x – y plane, and ζ is the microinertia density. Further, ρ is the fluid density, μ is the viscosity, κ is the microrotation parameter (also known as the coefficient of gyroviscosity or as the vortex viscosity) and γ is the spin-gradient viscosity. We follow the work of many recent authors by assuming that ζ is a constant. The Equations (1), (2), (3) and (4) are to be solved subject to:

$$\bar{v} \to 0, \quad \bar{u} = U, \quad \bar{N} = -n\frac{\partial \bar{u}}{\partial \bar{y}} \quad \text{on} \quad \bar{y} = 0 \tag{5a}$$

$$\bar{u} \to 0, \quad \bar{v} \to 0, \quad \bar{N} \to 0 \quad \text{as} \quad \bar{y} \to \infty \tag{5b}$$

In Equation (5a) we have followed Arafa and Gorla [11] in assigning a variable relation between $\bar{N}$ and the skin friction at the surface. The value $n = 0$, represents concentrated particle flows in which the microelements close to the wall are unable to rotate. The value $n = \frac{1}{2}$ is indicative of weak concentration, and when $n = 1$, is used for the modeling of turbulent boundary layer. We shall consider values of n which lie between these two extremes.

We introduce now the nondimensional variables:

$$x = \frac{\bar{x}}{l}, y = \frac{\bar{y}}{l}, u = \frac{\bar{u}}{U}, v = \frac{\bar{v}}{U}, p = \frac{\bar{p}}{\rho U^2}, N = \left(\frac{1}{U}\right)\bar{N} \tag{6}$$

and follow Ahmadi [10] to assume that γ is given by,

$$\gamma = \left(\mu + \frac{\kappa}{2}\right)\zeta, \tag{7}$$

We obtain from Equations (1) – (4) the following:

$$\frac{\partial u}{\partial x} + \frac{\partial v}{\partial y} = 0 \tag{8}$$

$$u\frac{\partial u}{\partial x} + v\frac{\partial u}{\partial y} = -\frac{\partial p}{\partial x} + \left(\frac{1+\mathrm{K}}{\mathrm{Re}}\right)\left(\frac{\partial^2 u}{\partial x^2} + \frac{\partial^2 u}{\partial y^2}\right) + \frac{\mathrm{K}}{\mathrm{Re}}\frac{\partial N}{\partial y} \tag{9}$$

$$u\frac{\partial v}{\partial x} + v\frac{\partial v}{\partial y} = -\frac{\partial p}{\partial y} + \left(\frac{1+\mathrm{K}}{\mathrm{Re}}\right)\left(\frac{\partial^2 v}{\partial x^2} + \frac{\partial^2 v}{\partial y^2}\right) - \frac{\mathrm{K}}{\mathrm{Re}}\frac{\partial N}{\partial x} \tag{10}$$

$$u\frac{\partial N}{\partial x} + v\frac{\partial N}{\partial y} = -\frac{\mathrm{K}}{\rho\zeta}\frac{l}{U}\left(2N + \frac{\partial u}{\partial y}\right) - \frac{\mathrm{K}}{\rho\zeta}\frac{l}{U}\frac{\partial N}{\partial x} + \left(\frac{1+\frac{\mathrm{K}}{2}}{\mathrm{Re}}\right)\left(\frac{\partial^2 N}{\partial x^2} + \frac{\partial^2 N}{\partial y^2}\right) \tag{11}$$

where K is the material parameter defined by $\mathrm{K} = \frac{\kappa}{\mu}$ and Re is the Reynolds number defined by $\mathrm{Re} = \frac{Ul}{v}$. If we take $\zeta = l^2$ as a reference length scale for ζ, then (11) becomes:

$$u\frac{\partial N}{\partial x} + v\frac{\partial N}{\partial y} = -\frac{\mathrm{K}}{\mathrm{Re}}\left(2N + \frac{\partial u}{\partial y}\right) - \frac{\mathrm{K}}{\mathrm{Re}}\frac{\partial N}{\partial x} + \left(\frac{1+\frac{\mathrm{K}}{2}}{\mathrm{Re}}\right)\left(\frac{\partial^2 N}{\partial x^2} + \frac{\partial^2 N}{\partial y^2}\right) \tag{12}$$

The boundary conditions (5) become:

$$v \to 0, \qquad u = 1, \qquad N = -n\frac{du}{dy} \quad \text{on} \quad y = 0 \tag{13a}$$

$$u \to 0, \qquad v \to 0, \qquad N \to 0 \quad \text{as} \quad y \to \infty \tag{13b}$$

Now we introduce the boundary layer variables:

$$X = x, \qquad Y = \mathrm{Re}^{\frac{1}{2}} y, \qquad U = u, \qquad V = \mathrm{Re}^{\frac{1}{2}} v, \qquad N = \mathrm{Re}^{\frac{1}{2}} N \tag{14}$$

into Equations (8), (9), (10) and (12) to obtain:

$$\frac{\partial U}{\partial X} + \frac{\partial V}{\partial Y} = 0 \tag{15}$$

$$U\frac{\partial U}{\partial X} + V\frac{\partial U}{\partial Y} = -\frac{\partial p}{\partial X} + (1+\mathrm{K})\left(\frac{1}{\mathrm{Re}}\frac{\partial^2 U}{\partial X^2} + \frac{\partial^2 U}{\partial Y^2}\right) + \mathrm{K}\frac{\partial N}{\partial Y} \tag{16}$$

$$\frac{1}{\mathrm{Re}}\left(U\frac{\partial V}{\partial X} + \frac{\partial V}{\partial Y}\right) = -\frac{\partial p}{\partial Y} + (1+\mathrm{K})\left(\frac{1}{\mathrm{Re}^2}\frac{\partial^2 V}{\partial X^2} + \frac{1}{\mathrm{Re}}\frac{\partial^2 V}{\partial Y^2}\right) - \frac{\mathrm{K}}{\mathrm{Re}^2}\frac{\partial N}{\partial X} \tag{17}$$

$$\begin{aligned}\mathrm{Re}^{-\frac{1}{2}}\left(U\frac{\partial N}{\partial X} + V\frac{\partial N}{\partial Y}\right) &= -\mathrm{K}\,\mathrm{Re}^{-\frac{1}{2}}\left(2N + \frac{\partial U}{\partial Y}\right) - \mathrm{K}\,\mathrm{Re}^{-\frac{3}{2}}\frac{\partial N}{\partial X} \\ &\quad + \left(1+\frac{\mathrm{K}}{2}\right)\mathrm{Re}^{-\frac{1}{2}}\left(\frac{1}{\mathrm{Re}}\frac{\partial^2 N}{\partial X^2} + \frac{\partial^2 N}{\partial Y^2}\right)\end{aligned} \tag{18}$$

Taking $\mathrm{Re} \to \infty$ as boundary layer approximation, we have:

$$\frac{\partial U}{\partial X} + \frac{\partial V}{\partial Y} = 0 \tag{19}$$

$$U\frac{\partial U}{\partial X} + V\frac{\partial U}{\partial Y} = -\frac{\partial p}{\partial X} + (1+\mathrm{K})\frac{\partial^2 U}{\partial Y^2} + \mathrm{K}\frac{\partial N}{\partial Y} \tag{20}$$

$$0 = -\frac{\partial p}{\partial Y} \tag{21}$$

$$U\frac{\partial N}{\partial X} + V\frac{\partial N}{\partial Y} = -\mathrm{K}\left(2N + \frac{\partial U}{\partial Y}\right) + \left(1+\frac{\mathrm{K}}{2}\right)\frac{\partial^2 N}{\partial Y^2} \tag{22}$$

The boundary conditions (13) reduce to:

$$V = 0, \quad U = 1, \quad N = -n\frac{\partial U}{\partial Y} \quad \text{on} \quad Y = 0 \tag{23a}$$

$$U = 0, \quad N \to 0 \quad \text{as} \quad Y \to \infty \tag{23b}$$

Equation (21) shows that $p = p(x)$ and Equation (20), on applying the boundary condition (23b), gives:

$$\frac{\partial p}{\partial X} = 0$$

Finally, we have the following boundary layer equations for the problem under consideration:

$$\frac{\partial U}{\partial X} + \frac{\partial V}{\partial Y} = 0 \tag{24}$$

$$U\frac{\partial U}{\partial X} + V\frac{\partial U}{\partial Y} = (1+K)\frac{\partial^2 U}{\partial Y^2} + \mathrm{K}\frac{\partial N}{\partial Y} \tag{25}$$

$$U\frac{\partial N}{\partial X} + V\frac{\partial N}{\partial Y} = \left(1+\frac{K}{2}\right)\frac{\partial^2 N}{\partial Y^2} - K\left(2\mathrm{N} + \frac{\partial U}{\partial Y}\right) \tag{26}$$

subject to the boundary conditions

$$V = 0, \quad U = 1, \quad N = -n\frac{\partial U}{\partial Y} \quad \text{on} \quad Y = 0$$
$$U = 0, \quad N \to 0 \quad \text{as} \quad Y \to \infty \tag{27}$$

we define the reduced stream function, f, the reduced gyration component, g, and the pseudo-similarity variable, η as:

$$f(X,\eta) = X^{-\frac{1}{2}}\psi, \quad g(X,\eta) = X^{\frac{1}{2}}N, \quad \eta = X^{-\frac{1}{2}}Y \tag{28}$$

where ψ is the stream function which satisfies:

$$\frac{\partial \psi}{\partial Y} = U, \quad \frac{\partial \psi}{\partial X} = -V \tag{29}$$

When the stream function ψ is introduced, the continuity Equation (24) is automatically satisfied. We obtain from (25) and (26):

$$(1+\mathrm{K})\frac{\partial^3 f}{\partial \eta^3} + \frac{1}{2}f\frac{\partial^2 f}{\partial \eta^2} + \mathrm{K}\frac{\partial g}{\partial \eta} = X\left(\frac{\partial f}{\partial \eta}\frac{\partial^2 f}{\partial X \partial \eta} - \frac{\partial f}{\partial X}\frac{\partial^2 f}{\partial \eta^2}\right) \tag{30}$$

$$\left(1+\frac{\mathrm{K}}{2}\right)\frac{\partial^2 g}{\partial \eta^2} + \frac{1}{2}\left(f\frac{\partial g}{\partial \eta} + \frac{\partial f}{\partial \eta}g\right) = \mathrm{K}X\left(2g + \frac{\partial^2 f}{\partial \eta^2}\right) + X\left(\frac{\partial f}{\partial \eta}\frac{\partial g}{\partial X} - \frac{\partial f}{\partial X}\frac{\partial g}{\partial \eta}\right) \tag{31}$$

with the boundary conditions

$$f = 0, \quad \frac{\partial f}{\partial \eta} = 1, \quad g = -n\frac{\partial^2 f}{\partial \eta^2} \quad \text{on} \quad \eta = 0 \tag{32a}$$

$$\frac{\partial f}{\partial \eta} \to 0, \quad g \to 0 \quad \text{as} \quad \eta \to \infty. \tag{32b}$$

Thus we have derived a set of parabolic partial differential equations which govern the development of the boundary layer, which in general, requires numerical solution.

Before presenting the computed results, it is convenient to draw attention to two cases for which Equations (30), (31) and boundary conditions (32) admit similarity solutions [8]. Similarity solution arises when $n = \frac{1}{2}$. We can take:

$$f(X,\eta) = f_0(\eta) \quad \text{and} \quad g(X,\eta) = g_0 = 0$$

where f_0 and g_0 are obtained from (30) and (31) as:

$$(1+\mathrm{K})f_0''' + \frac{1}{2}f_0 f_0'' + \mathrm{K}g_0' = 0 \tag{33}$$

$$g_0 = -\frac{1}{2}f_0'' \tag{34}$$

If we substitute Equation (34) into (33), we get:

$$\left(1+\frac{\mathrm{K}}{2}\right)f_0' + \frac{1}{2}f_0 f_0'' = 0 \tag{35}$$

subject to:

$$f_0(0) = 0, \quad f_0'(0) = 1 \quad \text{on} \quad \eta = 0$$
$$f_0'(\infty) \to 0 \quad \text{as} \quad \eta \to \infty \tag{36}$$

Now we set:

$$f_0(\eta) = \left(1+\frac{\mathrm{K}}{2}\right)^{\frac{1}{2}} \hat{f}_0(\hat{\eta}), \qquad \hat{\eta} = \left(1+\frac{\mathrm{K}}{2}\right)^{-\frac{1}{2}}\eta \tag{37}$$

Hence that Equation (35) reduces to:

$$\hat{f}_0''' + \frac{1}{2}\hat{f}_0\hat{f}_0'' = 0 \tag{38}$$

subject to:

$$\hat{f}_0(0) = 0, \quad \hat{f}'_0(0) = 1 \quad \text{on} \quad \hat{\eta} = 0$$
$$\hat{f}'_0(\infty) = 0 \quad \text{as} \quad \hat{\eta} \to \infty \tag{39}$$

Equations (38) and (39) describe the flow due to a moving flat plate in a quiescent fluid first described by Sakiadis [1].

Following Rees and Bassom [8], a second similarity solution arises when $K = 0$ for which

$$f(\eta) = \hat{f}(\eta) \quad \text{and} \quad g(\eta) = -nf''(0)e^{-\frac{1}{2}\int_0^\eta f(s)ds} \tag{40}$$

In this case, the flow field is unaffected by the microstructure of the fluid, and hence the gyration component is a passive quantity.

3.0 NUMERICAL SOLUTION

The full pseudo-similar boundary layer Equations (30) and (31) subject to the boundary conditions (32a, 32b) are solved numerically using the Keller-box method. In this method, the governing equations are first reduced to first order equation. We use the Newton's method to linearize the resulting nonlinear equations and lastly, we obtain the solutions using the block-elimination methods. In our present study, we have used the step sizes of $\Delta\eta = 0.05$ and $\Delta\xi = 0.05$. In all cases we choose $x_{\max} = 10$, $\xi_{\max} = 201$ and $y_{\max} = 6$, $\eta_{\max} = 121$. A solution is considered to converge when the difference between the input and output values of the $v(\xi,0)$ came within 10^{-10}.

Table 1 presents the comparison of f, f' and f'' between the present method and previously published data [1].

Figures (1) – (4) give some graphs of the characteristics of velocity profile f' and reduced gyration component g as a function of η at different streamwise locations for $K = 1$, $K = 0.5$ and $0 \le n \le 1$. Figures (1) and (2) show that $f'(\eta)$ decreases as increases.

Figures (3) and (4) display some profiles of the reduced gyration component, g as a function of η at various streamwise locations η with the parameter choice $K = 1$ and $K = 0.5$. Generally there is only a slight difference between these two figures. When $K = 1$ the value of g at $\eta = 1.0$ is 0.530515 and when $K = 0.5$ the value of g at $\eta = 1.0$ is 0.488204. On the other hand, the value of g at $\eta = 0$ when $K = 1$ and $K = 0.5$ varies with n.

Table 1 Comparison between Sakiadis [1] and the present method for the similar flow

	eta(η)	f	f′	f″
0.00	present	0.000000	1.000000	–0.443920
	(Sakiadis)	(0.00000)	(1.00000)	(–0.44375)
0.05	present	0.049445	0.977811	–0.443645
	(Sakiadis)	(0.04945)	(0.97782)	(–0.44347)
1.00	present	0.786152	0.587014	–0.358469
	(Sakiadis)	(0.78620)	(0.58715)	(–0.35831)
3.00	present	1.432201	0.143646	–0.109905
	(Sakiadis)	(1.43273)	(0.14401)	(–0.10984)
5.00	present	1.577469	0.029469	–0.023956
	(Sakiadis)	(1.57883)	(0.02995)	(–0.02392)
8.00	present	1.609876	0.002137	–0.002173
	(Sakiadis)	(1.61278)	(0.00267)	(–0.00216)

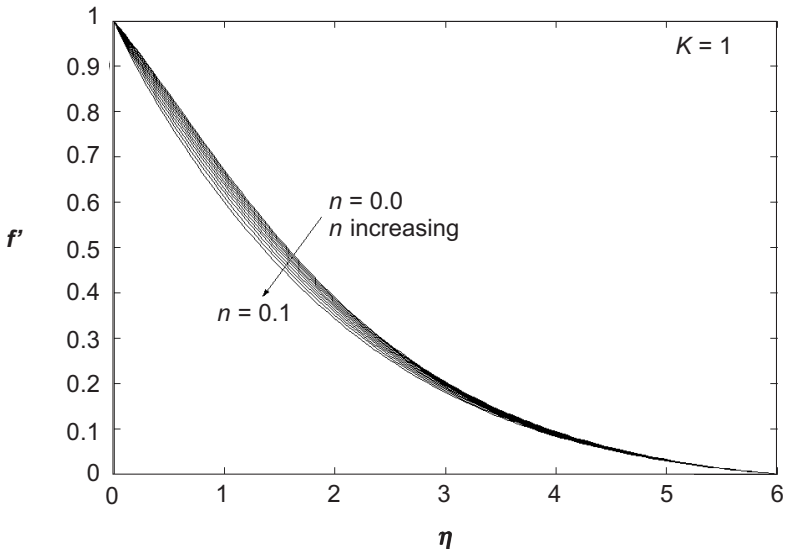

Figure 1 Profile of the reduced streamwise velocity f' as a function of η at different streamwise location for $K = 1$ and for $0 \le n \le 1$

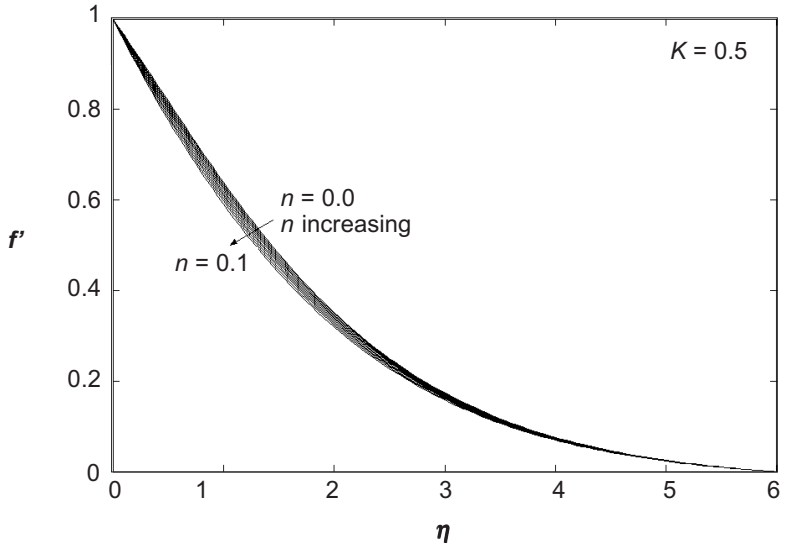

Figure 2 Profile of the reduced streamwise velocity f' as a function of η at different streamwise location for $K = 0.5$ and for $0 \leq n \leq 1$

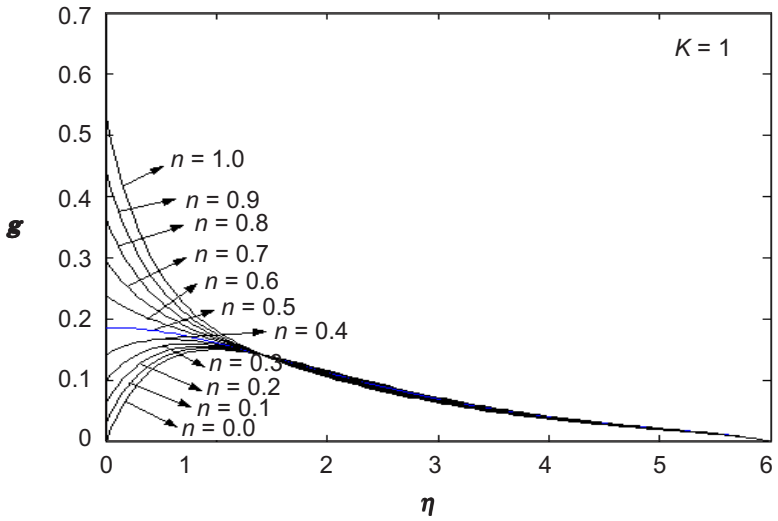

Figure 3 Profile of the reduced gyration component g as a function of η at different streamwise locations for $K = 1$ and for $0 \leq n \leq 1$

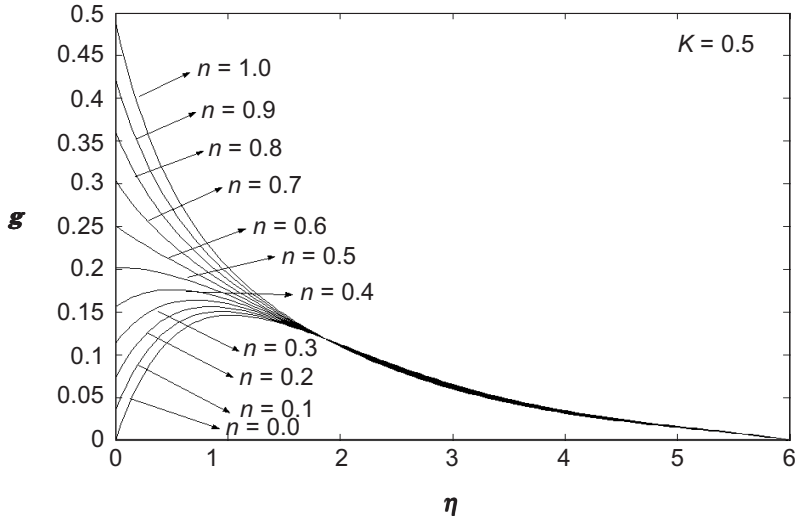

Figure 4 Profile of the reduced gyration component g as a function of η at different streamwise locations for $K = 0.5$ and for $0 \le n \le 1$

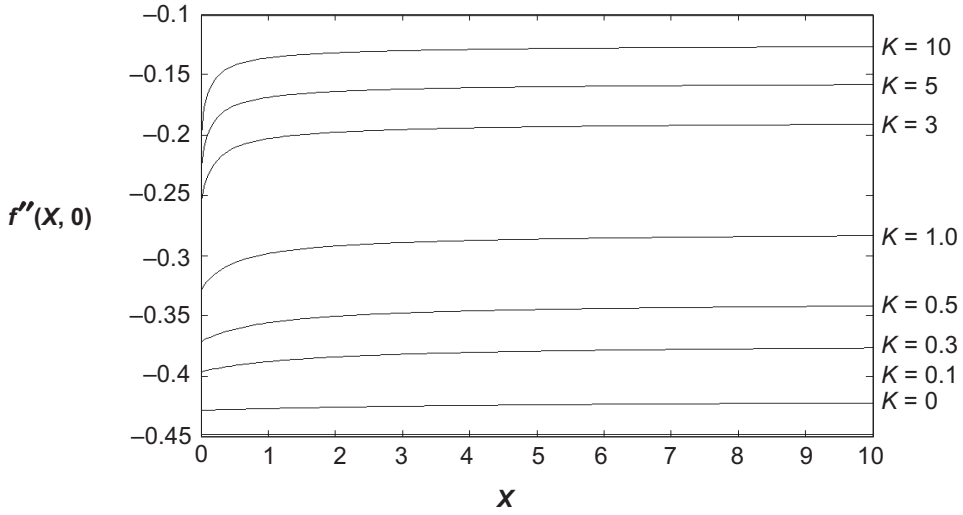

Figure 5 Development of the wall shear stress $f''(X, 0)$ as a function of X for $n = 0$ and for various values of K

Figures (5) - (8) illustrate the variation of the shear stress (or skin friction) and the rate of change of gyration component at the solid boundary with X. Figures (5) and (6) plot f'' at $\eta = 0$ as a function of X for various values of K, and for $n = 0$ and

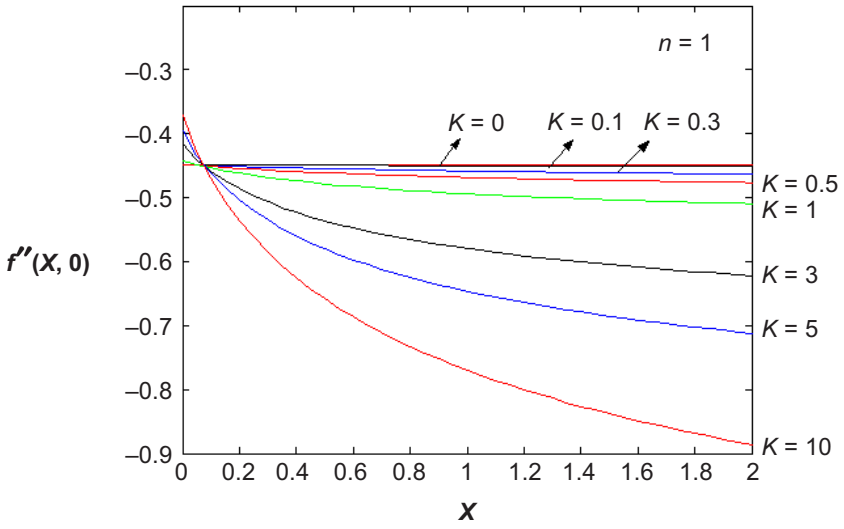

Figure 6 Development of the wall shear stress $f''(X, 0)$ as a function of X for $n = 1$ and for various values of K

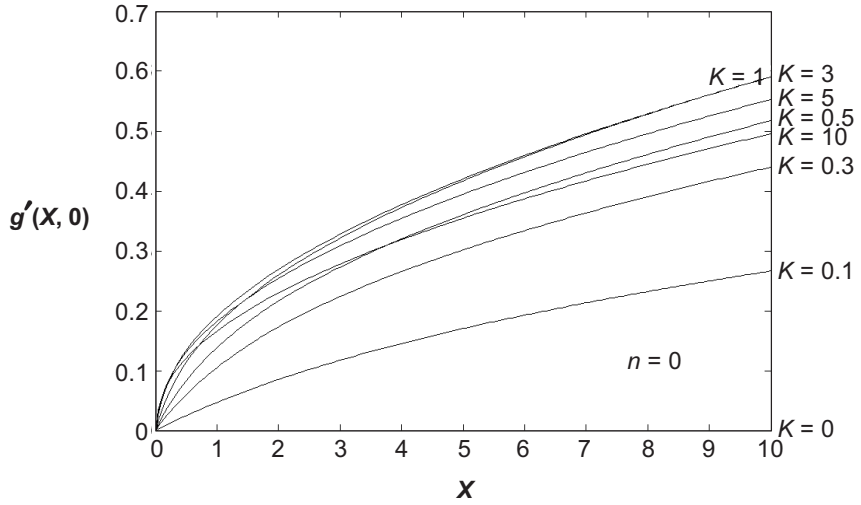

Figure 7 Development of the rate of change of the gyration component at the wall $g'(X, 0)$ as a function of X for $\eta = 0$ and for various values of K

$n = 0$. For fixed n, increasing value of f'' would seem to be associated with increasing value of K and when $K = 0$ the curves are very approximately or closed to being horizontal lines.

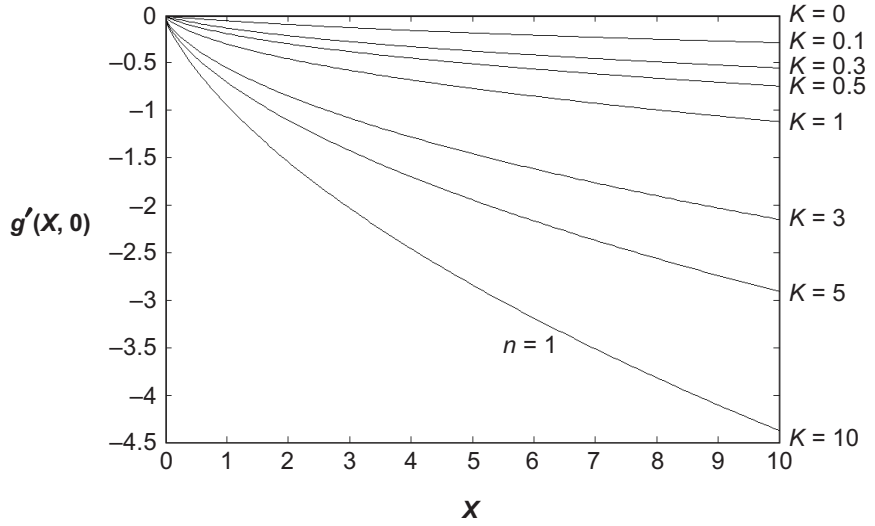

Figure 8 Development of the rate of change of the gyration component at the wall $g'(X, 0)$ as a function of X for $\eta = 1$ and for various values of K

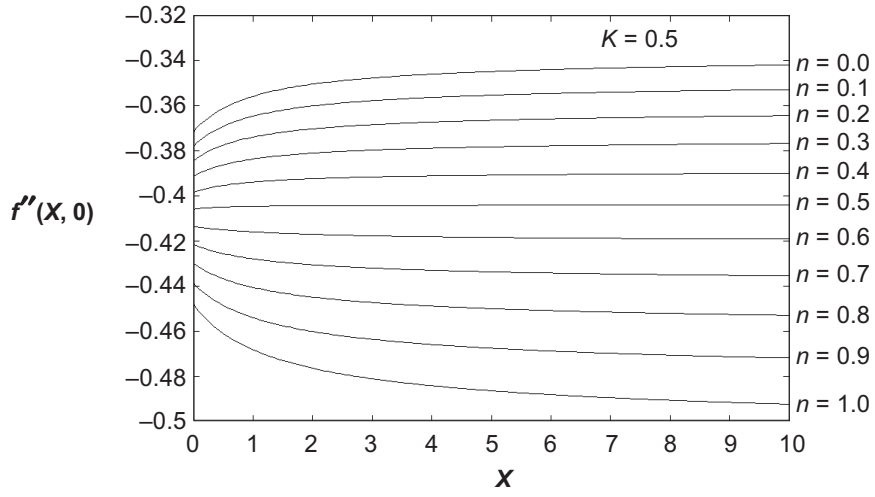

Figure 9 Development of the wall shear stress $f''(X, 0)$ as a function of X for $K = 0.5$ and a range of values of n

Figures (7) and (8) show the rate of change of the gyration component at the wall, $g''(X, 0)$ for different values of K.

Figures (9) - (12) consider the development of the wall shear stress, $f''(X, 0)$ and the rate of change of the gyration component at the wall, $g'(X, 0)$ with X. The figures

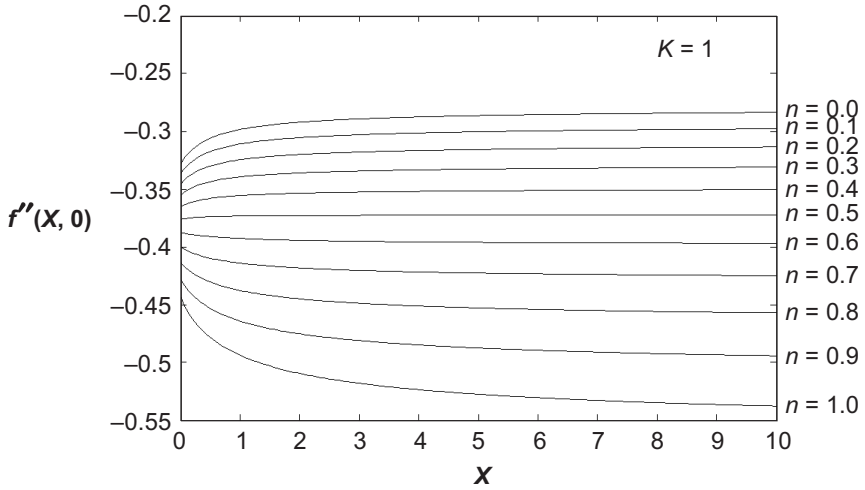

Figure 10 Development of the wall shear stress $f''(X, 0)$ as a function of X for $K = 1$ and a range of values of n

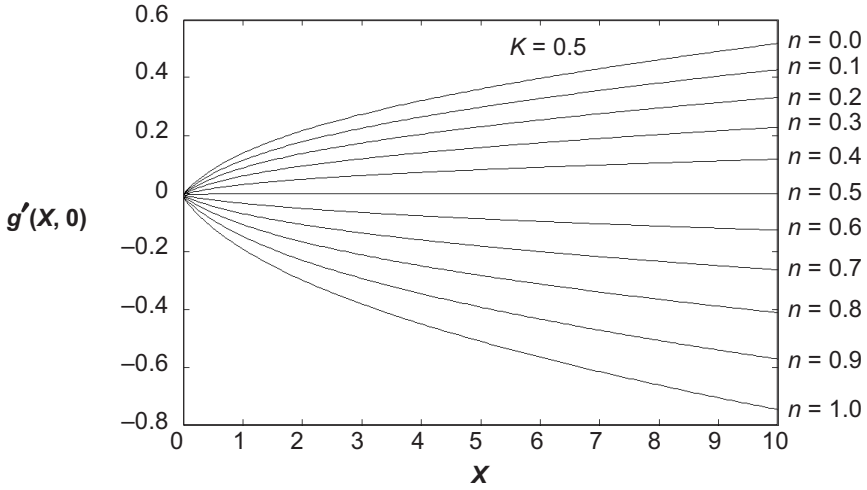

Figure 11 Development of function $g'(X, 0)$ as a function of X for $K = 0.5$ and a range of values of n

present the corresponding graphs when $K = 0.5$ and $K = 1$ is taken, and n is varied between 0 and 1. The similarity solution corresponding to $n = \frac{1}{2}$ is evident as a straight line in all these figures.

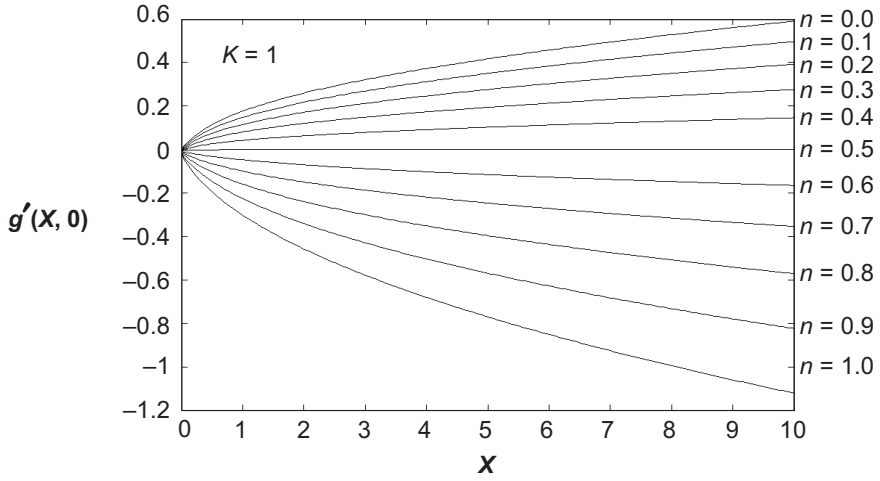

Figure 12 Development of function $g'(X, 0)$ as a function of X for $K = 1$ and a range of values of n

4.0 CONCLUSION

The governing boundary layer equations are solved numerically using an implicit finite difference scheme. Numerical results presented include the reduced velocity profiles, gyration component profiles and the development of wall shear stress or skin friction. These numerical results indicated that a near-wall contact layer develop as $X \to \infty$ but only if $n \neq \frac{1}{2}$. But, when either $n = \frac{1}{2}$ or $K = 0$, the solution is self-similar and there is no near-wall layer [8]. The results obtained, for the material parameter $K = 0$ (Newtonian fluid), are in excellent agreement with those obtained for viscous fluids. Further, the wall shear stress increases with increasing K. For fixed K, the wall shear stress decreases and the gyration component increases with increasing values of n, in the range $0 \leq n \leq 1$ where n is a ratio of the gyration vector component and the fluid shear stress at the wall.

REFERENCES

[1] Sakiadis, B. C. 1961. Boundary Layer Behavior Continuous Solid Surfaces: II. The Boundary Layer on a Continuous Flat Surface. *A.I.Ch. E. Journal*. 7: 221-225.

[2] Tsou, F., E. Sparrow, and R. Goldstein. 1967. Flow and Heat Transfer in the Boundary Layer on a Continuous Moving Surfaces. *Int. J. Heat and Mass Transfer*. 10: 219-235.

[3] Lee, W. W., and R. T. Davis. 1972. Laminar Boundary Layer on Moving Continuous Surfaces. *Chemical Eng. Science*. 27: 2129-2149.

[4] Noor Afzal. 1996. Turbulent Boundary Layer on a Moving Continuous Plate. *Fluid Dynamic Research*. 17: 181-194.

[5] Eringen, A. C. 1964. Simple Microfluids. *Int. J. Engng. Sci*. 2: 205.

[6] Eringen, A. C. 1966. Theory of Micropolar Fluid. *J. Math. Mech*. 16: 1-18.

[7] Ariman, T., M. A. Turk, and N. D. Sylvester. 1973. Microcontinuum Fluid Mechanics- a Review. *Int. J. Engng. Sci.* 11: 905-930.
[8] Rees, D. A. S., and A. P. Bassom. 1996. The Blasius Boundary Layer Flow of a Micropolar Fluid. *Int. J. Engng. Sci.* 34: 113-124.
[9] Soundalgekar, V. M., and H. S. Takhar. 1983. Flow of Micropolar Fluid Past a Continuously Moving Flat Plate. *Int. J. Engng. Sci.* 21: 961-905.
[10] Ahmadi, G. 1976. Self Similar Solution of Incompressible Micropolar Boundary Layer Flow over a Semi Infinite Plate. *Int. J. Engng. Sci.* 14: 639-646.
[11] Arafa, A. A., and R. S. R. Gorla. 1992. Mixed Convection Boundary Layer Flow of a Micropolar Fluid Along Vertical Cylinders and Needles. *Int. J. Engng. Sci.* 30: 1745-1751.

NOMENCLATURE

Roman Letters

f – Reduced stream function

f_0 – Reduced stream function for $n = \frac{1}{2}$

$\hat{f}$ – Reduced stream function for the classical Blasius boundary-layer flow

g – Reduced gyration component

g_0 – Reduced gyration component for $n = \frac{1}{2}$

ζ – Microinertia density

j_0 – Reference value of the microinertia density

K – Ratio of the gyroviscosity and the fluid viscosity

l – Length scale

n – Ratio of the gyration vector component and the fluid shear at a solid boundary

N – The gyration vector component perpendicular to the x-y plane

p – Pressure

Re – Reynolds number, $\frac{\rho U_o l}{\mu}$

v – Fluid velocity component in y-direction

x – Coordinate along the plate

$\bar{x}$ – Dimensionless coordinate x

y – Coordinate normal to the plate

$\bar{y}$ – Dimensionless coordinate y

X, Y – Nondimensional streamwise and cross-stream Cartesian coordinates

$\overline{u}$ – Dimensionless velocity u

u – Fluid velocity component in x-direction

U – Free stream velocity

$\overline{v}$ – Dimensionless velocity v

Greek Letters

δ – Boundary layer thickness

η – Pseudo-similarity variable

$\hat{\eta}$ – Scaled pseudo-similarity variable

γ – Spin-gradient viscosity

μ – Dynamic viscosity

κ – Coefficient of gyroviscosity

υ – Kinematic viscosity

ξ – Transformed streamwise coordinate

ρ – Density of the fluid

ψ – Stream function

θ – Momentum thickness

Superscripts

$'$ – Differentiation with respect to

$^-$ – Dimensional variables